Optimization of a polymer four-port microring optical router with three channel wavelengths*

LUO Qian-qian (罗倩倩), **HUANG Xiao-liang** (黄小亮), **ZHENG Chuan-tao** (郑传涛)**, **and ZHANG Da-ming** (张大明)

State Key Laboratory on Integrated Optoelectronics, College of Electronic Science and Engineering, Jilin University, Changchun 130012, China

(Received 7 November 2013; Revised 10 December 2013)

Optimization and simulation are performed for a polymer four-port microring optical router with three channel wavelengths, which contains four-group basic routing elements with two different ring radii. In terms of microring resonance theory, coupled mode theory and transfer matrix method, expressions of output power of basic routing element and optical router are derived. In order to realize single-mode propagation, low optical transmission loss and phase match between microring waveguide and channel waveguide, the device parameters are optimized. With the selected three channel wavelengths of 1550 nm, 1552 nm and 1554 nm, characteristics are calculated and analyzed, including output spectrum, insertion loss and crosstalk. Simulation results indicate that the device has 12 possible I/O routing paths, the insertion losses of three channel wavelengths along their routing paths are within the range of 0.02−0.61 dB, the maximum crosstalk between the on-port along each routing path and other off-ports is less than −39 dB, and the device footprint size is ~0.13 mm^2. Based on the proposed structure, through proper selection on ring radius, the routing structure can also be used for other channel wavelengths. Therefore, the designed structure shows wide applications in integrated optical networks-on-chip (NoC).

Document code: A **Article ID:** 1673-1905(2014)02-0091-5

DOI 10.1007/s11801-014-3213-9

In the photonic networks-on-chip (NoC)[1-4], the optical router[5,6], consisting of optical waveguide and optical switches, can realize the routing optical signals to the designated destination. Mach-Zehnder interferometer (MZI)[7], directional coupler (DC)[8], and microring resonators (MRRs) are promising candidates for very large scale integrated optoelectronic circuits[9-11]. Passive optical router, also named wavelength router, is an alluring option for no power consumption[6,12]. In this paper, using polymer materials, we propose a kind of four-port passive optical router. For obtaining small ring radius, air, with a refractive index of only 1.0, is chosen as the cladding material besides the polymer waveguide core (refractive index of 1.59). Under this condition, the radius of the microring resonator is decreased to 13.7−14.0 μm. This will be helpful for decreasing device footprint size.

The structure model of the designed four-port polymer optical router is shown in Fig.1(a). The cross-coupling two-microring resonators labeled in the same color are with the same radius, i.e. they have the same resonance wavelength. The resonance wavelengths of the microrings are λ_1 and λ_2, and the input channel wavelengths are λ_1, λ_2 and λ_3. The two ports marked by I_i and O_i (i = 0−3) locate at each of the four directions, including north (N), west (W), south (S) and east (E). Because of the symmetry of the two ports between I_0 and I_3 and that between I_1 and I_2, with the same wavelength of light input into each pair of ports, the same transmission spectrum can be derived from the imaging output ports. The length of input and output waveguides of each port is L_1=100 μm, and the center to center spacing is designed to be L_2=100 μm.

The basic cross-coupling two-microring resonator is shown in Fig.1(b), which consists of a horizontal channel waveguide, a vertical channel waveguide and two microrings (with the same radius of R) cross-coupled with the two channels. The waveguide cross-section between MRR waveguide and channel waveguide is shown in Fig.1(c). The distance between coupling planes of S_1 and S_3 and that between S_2 and S_4 are both L_{CC}. For obtaining the same mode propagation constants, the two core

* This work has been supported by the National Natural Science Foundation of China (Nos.61107021, 61177027 and 61077041), the Ministry of Education of China (Nos.20110061120052 and 20120061130008), the China Postdoctoral Science Foundation Funded Project (Nos.20110491299 and 2012T50297), the Science and Technology Department of Jilin Province of China (No.20130522161JH), and the Special Funds of Basic Science and Technology of Jilin University (Nos.201103076 and 200905005).

** E-mail: zhengchuantao@jlu.edu.cn

widths of MRR waveguide and channel waveguide are slightly different. Around 1550 nm, the refractive index n_{10} of the polymeric waveguide core[13] is 1.590 and the bulk amplitude attenuation coefficient is α_{10}=0.25 dB/cm; the refractive index n_{20} of the polymer buffer layer[14] is 1.461, and its bulk amplitude attenuation coefficient is α_{20}= 0.25 dB/cm; the refractive index n_{30} of the left/right cladding (air) is 1.000 and the bulk amplitude attenuation coefficient is α_{30}=0. E_{00}^{y} is selected as the fundamental propagation mode.

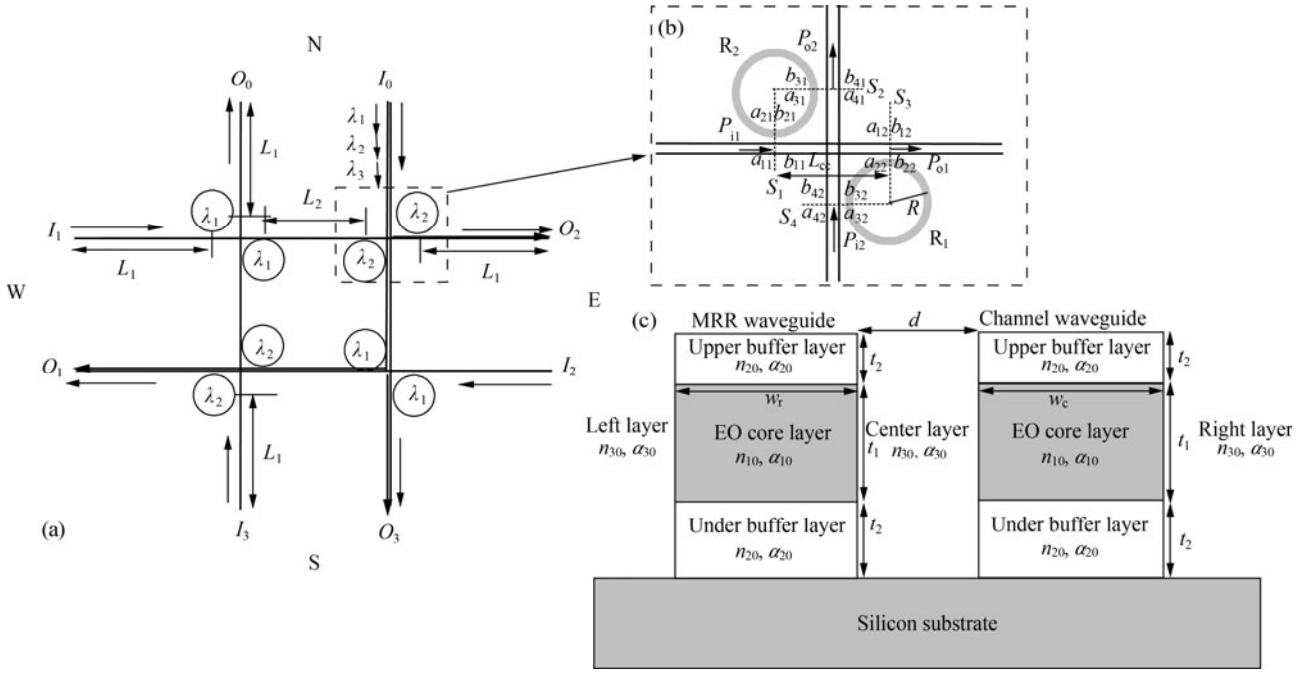

Fig.1 (a) Structure of the polymer four-port optical router; (b) Structure of the polymer cross-coupling two-ring resonator; (c) Cross-section view over the coupling plane between MRR waveguide and channel waveguide

Considering the symmetry of the basic cross-coupling two-microring resonator (Fig.1(b)), we only analyze the case of light input into the horizontal port. At the coupling plane S_1 between microring R_2 and horizontal channel, a_{11}, b_{11} and a_{21}, b_{21} are the input and output light amplitudes of the horizontal channel waveguide and microring waveguide, respectively. Over other three coupling planes S_2, S_3 and S_4, a_{21}, b_{21}, a_{31}, b_{31}, a_{41}, b_{41}, a_{12}, b_{12}, a_{22}, b_{22}, a_{32}, b_{32}, a_{42} and b_{42} are also defined and labeled in Fig.1(b). The relation among the four amplitudes over each plane can be described by the following transfer matrices

$$\begin{bmatrix} a_{2i} \\ b_{2i} \end{bmatrix} = \frac{1}{\mathrm{j}\kappa_{\mathrm{CR}}} \begin{bmatrix} t_{\mathrm{CR}} & -1 \\ 1 & -t_{\mathrm{CR}} \end{bmatrix} \begin{bmatrix} a_{1i} \\ b_{1i} \end{bmatrix},$$

$$\begin{bmatrix} a_{4i} \\ b_{4i} \end{bmatrix} = \frac{1}{\mathrm{j}\kappa_{\mathrm{CR}}} \begin{bmatrix} t_{\mathrm{CR}} & -1 \\ 1 & -t_{\mathrm{CR}} \end{bmatrix} \begin{bmatrix} a_{3i} \\ b_{3i} \end{bmatrix}, \ i=1,2. \tag{1}$$

Besides, outside the coupling planes, optical propagation in resonators can be expressed as

$$\begin{bmatrix} a_{21} \\ b_{21} \end{bmatrix} = \begin{bmatrix} 0 & \exp(-\mathrm{j}\phi_1) \\ \exp(\mathrm{j}\phi_2) & 0 \end{bmatrix} \begin{bmatrix} a_{31} \\ b_{31} \end{bmatrix},$$

$$\begin{bmatrix} a_{22} \\ b_{22} \end{bmatrix} = \begin{bmatrix} 0 & \exp(-\mathrm{j}\phi_2) \\ \exp(\mathrm{j}\phi_1) & 0 \end{bmatrix} \begin{bmatrix} a_{32} \\ b_{32} \end{bmatrix}, \tag{2}$$

$$a_{41} = b_{42}\exp(-\mathrm{j}\psi_2), \tag{3}$$

$$a_{12} = b_{11}\exp(-\mathrm{j}\psi_2), \tag{4}$$

$$a_{42} = 0, \tag{5}$$

with $\phi_1 = 1.5\pi R(\beta_{\mathrm{R}} - \mathrm{j}\alpha_{\mathrm{R}})$, $\phi_2 = 0.5\pi R(\beta_{\mathrm{R}} - \mathrm{j}\alpha_{\mathrm{R}})$, $\psi_2 = L_{\mathrm{CC}}(\beta_{\mathrm{C}} - \mathrm{j}\alpha_{\mathrm{C}})$, where $\beta_{\mathrm{C}} = (2\pi/\lambda)n_{\mathrm{C}}$ and $\beta_{\mathrm{R}} = (2\pi/\lambda)n_{\mathrm{R}}$ are the mode propagation constants of channel waveguide and MRR waveguide, respectively, which should be approximately equal for phase matching, and α_{C} and α_{R} are the mode amplitude loss coefficients of channel waveguide and MRR waveguide, respectively. From Eqs.(1)–(5), the amplitude transfer function of the basic routing element is obtained by

$$U = \frac{b_{12}}{a_{11}} = \frac{t_{\mathrm{CR}} f_1 \left\{ f_1 - \kappa_{\mathrm{CR}}^2 \exp[-\mathrm{j}(\varphi_1 + \varphi_2)] \right\}}{f_2}, \tag{6}$$

$$V = \frac{b_{41}}{a_{11}} = -\frac{\kappa_{\mathrm{CR}}^2 f_2 \exp(-\mathrm{j}\phi_2)}{f_1 f_2} + \frac{t_{\mathrm{CR}}^2 \kappa_{\mathrm{CR}}^2 \exp\left[-\mathrm{j}(\phi_1 + 2\psi_2)\right] \left\{ f_1 - \kappa_{\mathrm{CR}}^2 \exp\left[-\mathrm{j}(\phi_1 + \phi_2)\right] \right\}^2}{f_1 f_2}, \tag{7}$$

where $f_1 = 1 - t_{\mathrm{CR}}^2 \exp\left[-\mathrm{j}(\phi_1 + \phi_2)\right]$, $f_2 = f_1^2 - \kappa_{\mathrm{CR}}^4 \exp\left[-\mathrm{j}\times(2\phi_1 + 2\psi_2)\right] \left\{ f_1 + t_{\mathrm{CR}}^2 \exp\left[-\mathrm{j}(\phi_1 + \phi_2)\right] \right\}$. The output power from the two ports (defined as through port and drop port) in dB form can be expressed as

$$P_{\mathrm{B}}=10\lg\left(\left|U\right|^2\right),$$
$$P_{\mathrm{D}}=10\lg\left(\left|V\right|^2\right). \quad (8)$$

For the convenience in the following analysis, we define transfer functions as follows. When the light with wavelength λ is input into the basic routing element with resonance wavelength λ_i, define $P_{\mathrm{B}\lambda_i}^{\lambda}$ as the output power of the through-port, and $P_{\mathrm{D}\lambda_i}^{\lambda}$ as that of the drop-port. On the basis of the symmetry between the two ports of I_0 and I_3 and that between the two ports of I_1 and I_2, with the same input wavelength, the identical insertion loss and crosstalk are derived for the corresponding output ports. Under the case of the light with any wavelength input into port i, the output power from another port, defined as $P_{\mathrm{in},i}^{\mathrm{out},j}$, can be derived below. For example, under the case of light with any wavelength input into port I_0,

$$P_{\mathrm{in},0}^{\mathrm{out},0}(\lambda)=(2L_1+3L_2)\cdot 2\alpha_{\mathrm{C}}(\lambda)+$$
$$P_{\mathrm{B}\lambda_2}^{\lambda}+P_{\mathrm{D}\lambda_1}^{\lambda}+P_{\mathrm{D}\lambda_1}^{\lambda}+P_{\mathrm{B}\lambda_1}^{\lambda}, \quad (9)$$
$$P_{\mathrm{in},0}^{\mathrm{out},1}(\lambda)=(2L_1+2L_2)\cdot 2\alpha_{\mathrm{C}}(\lambda)+2P_{\mathrm{B}\lambda_2}^{\lambda}+P_{\mathrm{D}\lambda_1}^{\lambda}, \quad (10)$$
$$P_{\mathrm{in},0}^{\mathrm{out},2}(\lambda)=2L_1\cdot 2\alpha_{\mathrm{C}}(\lambda)+P_{\mathrm{D}\lambda_2}^{\lambda}, \quad (11)$$
$$P_{\mathrm{in},0}^{\mathrm{out},3}(\lambda)=(2L_1+L_2)\cdot 2\alpha_{\mathrm{C}}(\lambda)+P_{\mathrm{B}\lambda_2}^{\lambda}+P_{\mathrm{B}\lambda_1}^{\lambda}. \quad (12)$$

Other cases can be similarly treated.

Supposing the upper/under confined layer is half-infinite (in practical design, this thickness is taken as $t_2 > 2.5$ μm), Fig.2 shows the curves of effective refractive indices of E_{00}^{y}, E_{01}^{y} and E_{10}^{y} modes versus MRR waveguide core width w_{r}, where the core thickness and width are equal, that is, $w_{\mathrm{r}}=t_1$, and the wavelength is 1550 nm. It can be found that in order to realize single-mode propagation, the core thickness should satisfy 1.2 μm$<w_{\mathrm{r}}=t_1<$ 2.1 μm, and during design we select $w_{\mathrm{r}}=t_1=1.7$ μm. Under the case of considering bending effect, the effective refractive index of E_{00}^{y} mode is larger than that without considering bending effect, as shown in the figure. The effective refractive index of E_{00}^{y} mode of the channel waveguide versus core width w_{c} is also shown in Fig.2. For ensuring the effective refractive index of the microring waveguide (n_{R}) and that of the channel waveguide (n_{C}) are the same, the width of the channel waveguide is taken as $w_{\mathrm{c}}=2.03$ μm. The coupling gap d between MRR waveguide and channel waveguide is designed to be 0.14 μm, and the transmittance coefficient t_{CR} and coupling coefficient κ_{CR} between MRR waveguide and channel waveguide are 0.99624 (at 1550 nm) and 0.08664 (at 1550 nm), respectively.

The designed four-port optical router is operated at three kinds of wavelengths, and in this paper 1550 nm, 1552 nm and 1554 nm are selected. Accordingly, the four-port device requires two kinds of basic routing elements, numbered by #1 (resonance at 1550 nm) and #2 (resonance at 1552 nm), respectively. For convenience, we define the channels with the wavelengths of 1550 nm, 1552 nm and 1554 nm as channel #1, #2 and #3, respectively. The first thing is to decide the two ring radii for realizing the routing operation of these three channel wavelengths, and they should satisfy the resonance equation $2\pi R n_{\mathrm{R}}=m\lambda$, where m is the resonance order and n_{R} is the effective index of the curved waveguide. In Fig.3, the resonance order is m = 85. One can find that the bending radius of microring increases and the mode effective refractive index decreases, as the resonance wavelength increases. In practical design, bending radius cannot be too large, otherwise it will cause the increase of optical loss. In our design, the resonance wavelength and corresponding bending radius of the two kinds of microrings are 13.756 μm and 13.775 μm. When the bending radii are taken as those values, the mode amplitude bending losses are both dropped below 10^{-4} dB/cm.

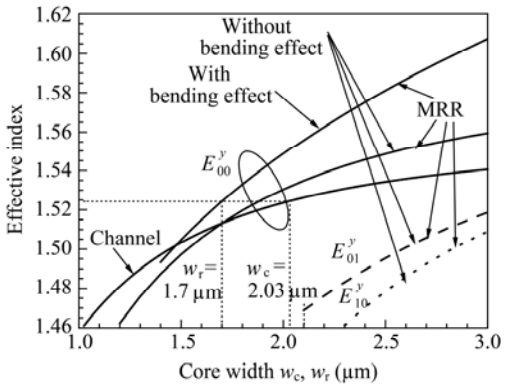

Fig.2 Curves of effective refractive indices of different modes propagating in MRR waveguide and channel waveguide versus core width

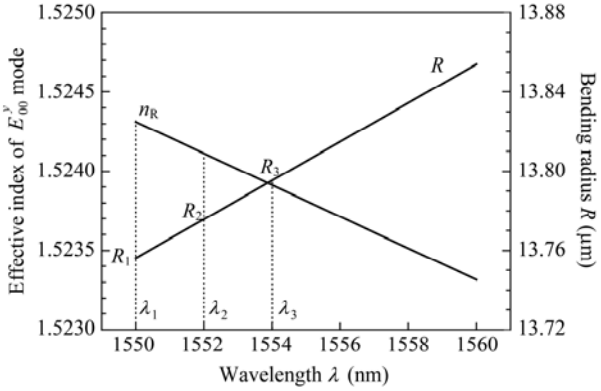

Fig.3 Curves of ring radius and effective index of fundamental mode versus wavelength for the MRR waveguide considering bending effect

The transmission spectra of 12 possible paths (from I_i to O_j, $i \neq j$) are shown in Fig.4. We can see that the output power of U-turn paths is so small that it can be neglected. When optical signals with the wavelengths of λ_1, λ_2 and λ_3 are injected into port I_0 together, they will be routed to the output ports of O_1, O_2 and O_3, respectively. Similarly, the situations of optical signals injected into ports I_1, I_2 and I_3 can be analyzed. Based on Fig.4, the wavelength routing principle of the optical router is depicted in Tab.1, which illustrates that the optical signal

with wavelength of λ_i(i=1,2,3) has a specific input-output path selected by microring routing elements.

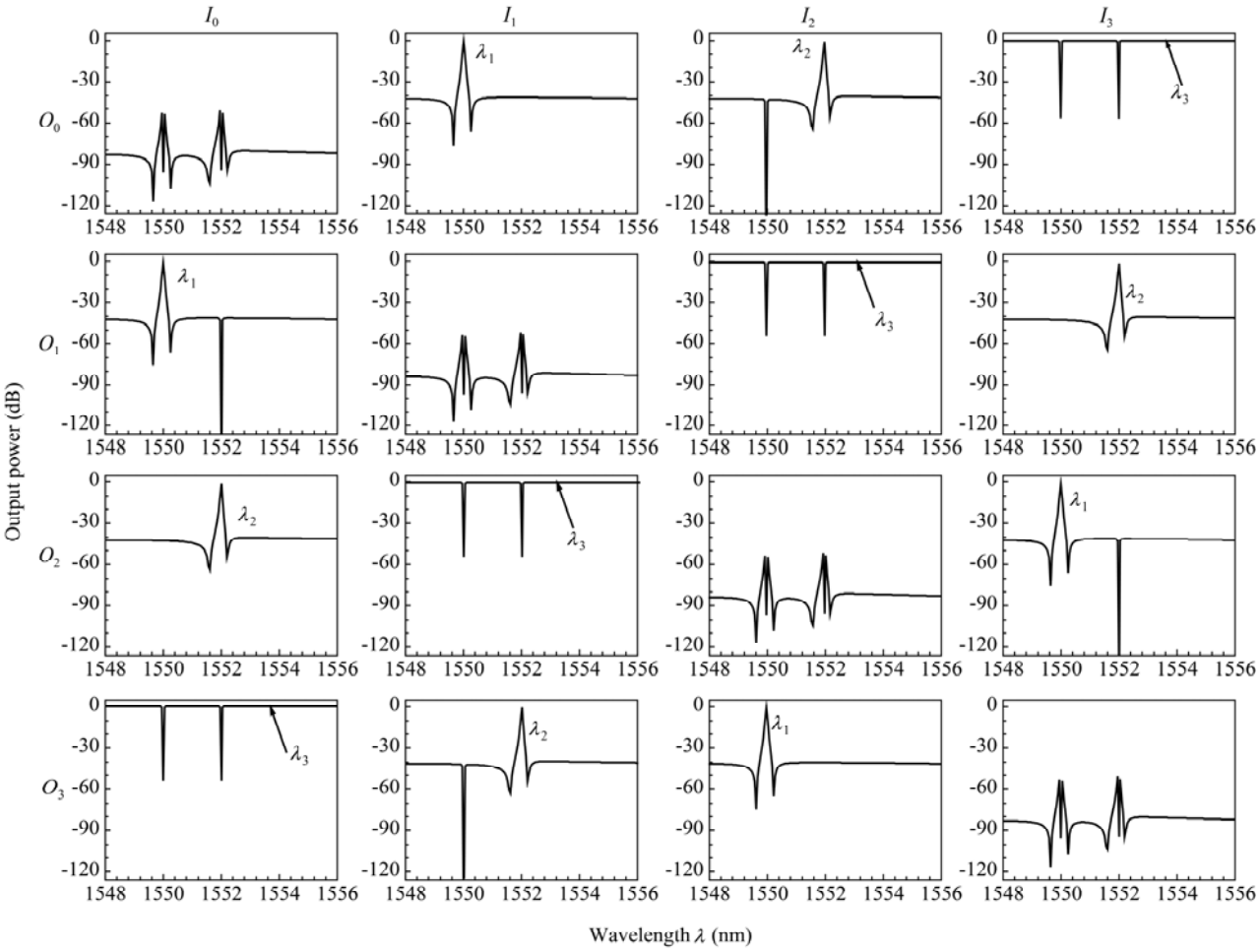

Fig.4 Optical spectra of 16 routing paths of the four-port optical router under different input/output routing operations

Tab.1 Routing paths of the one-stage four-port optical router

		Output			
		O_0	O_1	O_2	O_3
Input	I_0	/	λ_1	λ_2	λ_3
	I_1	λ_1	/	λ_3	λ_2
	I_2	λ_2	λ_3	/	λ_1
	I_3	λ_3	λ_2	λ_1	/

The insertion losses under the cases of light input into different ports and output from the appointed ports (on-port) are depicted in Figs.5(a) and (b). It can be found that the insertion losses of all channel wavelengths are approximately uniform, whose maximum value is 0.61 dB and minimum value is 0.02 dB. Fig.5 also shows the crosstalks of all channel wavelengths under the cases of light signals input into different ports. As shown in Fig.5(a), when light signals (λ_1, λ_2, λ_3) are input into port I_0 or I_3, the crosstalks of the three channel wavelengths are –41.28 dB, –53.00 dB and –40.04 dB in that order. As shown in Fig.5(b), when light signals (λ_1, λ_2, λ_3) are input into port I_1 or I_2, the crosstalks of the three channel wavelengths are –52.87 dB, –39.97 dB and –40.05 dB, respectively.

For the cross-coupling two-microring resonators with the radius of R_i, the distance between two horizontal or vertical coupling planes can be calculated by $L_{CC,i} = 2\left(R_i + \frac{w_r}{2} + d + \frac{w_c}{2}\right)$. Therefore, the device length in both directions is $L_H = L_W = 2L_1 + L_2 + \sum_{i=1}^{2} L_{CC,i} = 362.1$ μm. The footprint size is about $L_W \times L_H$=0.13 mm^2.

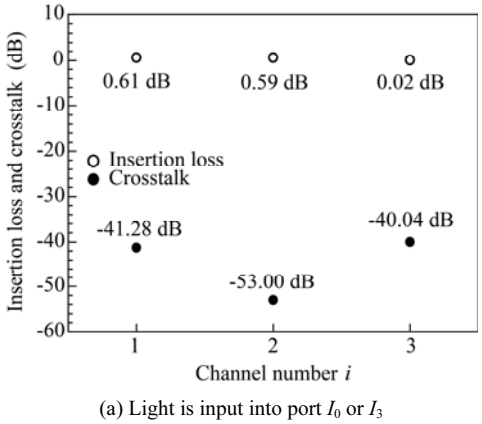

(a) Light is input into port I_0 or I_3

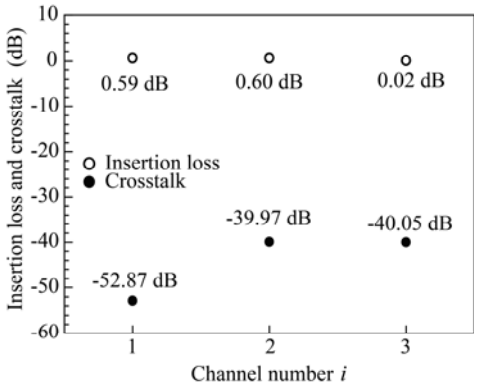

(b) Light is input into port I_1 or I_2

Fig.5 The insertion losses of definite routing port under on state and the maximum crosstalk of this on-port relative to other off-ports

In conclusion, we propose a four-port polymer optical router consisting of four cross-coupling microring resonators, and proper structural parameters are selected through optimization. It can route three channel wavelengths and includes 12 possible I/O routing paths. The insertion losses of all channel wavelengths along their routing paths are within the range of 0.02–0.61 dB, the maximum crosstalks between the on-port along each routing path and other off-ports are less than –39 dB, and the device also has ultra-compact footprint size of only 0.13 mm^2.

References

[1] B. G. Lee, A. Biberman, P. Dong, M. Lipson and K. Bergman, IEEE Photon. Technol. Lett. **20**, 767 (2008).

[2] A. B. Miller, Device Requirements for Optical Interconnects to Silicon Chips, Proc. IEEE **97**, 1166 (2009).

[3] K. H. Mo, Y. Y. Ye, X. W. Wu, W. Zhang, W. C. Liu and J. Xu, A Hierarchical Hybrid Optical-electronic Network-on-chip, IEEE Annual Symposium on VLSI, 327 (2010).

[4] A. Shacham, K. Bergman and L. P. Carloni, IEEE Trans. Comput. **57**, 1246 (2008).

[5] A. Biberman, B. G. Lee, N. S. Droz, M. Lipson and K. Bergman, IEEE Photon. Technol. Lett. **22**, 926 (2012).

[6] X. F. Tan, M. Yang, L. Zhang, Y. T. Jiang and J. Y. Yang, J. Lightwave Technol. **30**, 368 (2012).

[7] C. T. Zheng, C. S. Ma, X. Yan and D. M. Zhang, Appl. Phys. B **102**, 831 (2011).

[8] R. Wang, C. T. Zheng, Q. Song, L. Liang, C. S. Ma, Z. C. Cui and D. M. Zhang, Opt. Commun. **285**, 1103 (2012).

[9] H. X. Gu, K. H. Mo, J. Xu and W. Zhang, A Low-power Low-cost Optical Router for Optical Networks-on-chip in Multiprocessor Systems-on chip, Proc. IEEE Comput. Soc. Annu. Symp. 19 (2009).

[10] R. Ji, L. Yang, L. Zhang, Y. Tian, J. Ding, H. Chen, Y. Lu, P. Zhou and W. Zhu, Opt. Exp. **19**, 18945 (2011).

[11] R. Min, R. Q. Ji, Q. S. Chen, L. Zhang and L. Yang, J. Lightwave Technol. **30**, 3736 (2012).

[12] T. Hu, H. Y. Qiu, P. Yu, C. Qiu, W. J. Wang, X. Q. Jiang, M. Yang and J. Y. Yang, Opt. Lett. **36,** 4710 (2011).

[13] G. Y. Xu, Z. F. Liu, J. Ma, B. Y. Liu, S. T. Ho, L. Wang, P. W. Zhu, T. J. Marks, J. D. Luo and A. K. Y. Jen, Opt. Exp. **13**, 7380 (2005).

[14] C. Pitois, S. Vukmirovic, A. Hult, D. Wiesmann and M. Robertsson, Macromolecules **32**, 2903 (1999).